

Fabrication of Gelatin Microgels by a “Cast” Strategy for Controlled Drug Release

Anhe Wang, Yue Cui, Junbai Li,* and Jan C. M. van Hest*

In this paper, we propose a “casting” strategy to prepare intrinsically fluorescent, uniform and porous gelatin microgels with multi-responsiveness. Gelatin microgels with tunable size were obtained by copying the structure of a porous CaCO_3 template. The diameter of the gelatin microgels was sensitive to salt concentration and pH. Doxorubicin and Rhodamine B as model drugs were loaded into the microgels via electrostatic interaction and release of the payload was triggered by changing the salt concentration and pH, respectively. Cell experiments demonstrated that the gelatin microgels had an excellent biocompatibility and biodegradability. The merits of gelatin microgels such as tunable size, biocompatibility, and stimulus responsive upload and release of positively charged small molecules will permit the microgels as excellent carriers for drug delivery. The whole manufacturing process is furthermore environmental-friendly involving no organic solvents and surfactants.

groups which can be utilized for further bioconjugation with for example cell targeting agents.^[10,11] Currently, different methods have been developed to prepare gelatin gels at the micro- and nanoscale size, such as photolithographic and micro-molding methods, microfluidic preparation, spray drying, freeze drying, single coacervation, complex coacervation and emulsification.^[11,14] In order to obtain uniform nano- and microgels the above-mentioned methods require either organic solvents, surfactants and/or expensive processing equipments.^[11,14] The residual organic solvents and surfactants used in these processes of preparation may affect the biocompatibility of the gelatin nano- and microgels.^[15–18] Meanwhile, the gelatin microgels obtained by the above-mentioned methods have a relatively

1. Introduction

Gelatin is an extensively used natural material because of its many advantageous properties, such as low-toxicity, biodegradability, biocompatibility and non-immunogenicity. It has been intensively studied for many years and has been widely applied in pharmacy, food and cosmetics.^[1–6] Particularly, gelatin nano- and microgels have attracted much attention in tissue engineering and drug delivery applications in recent years.^[7–13] Additionally, gelatin gels possess a high content of functional

smooth surface and compact structure, which limits the absorption and subsequent release of drugs. Therefore, it is urgently needed to develop an environmentally friendly method for the preparation of gelatin microgels with a porous morphology for improved drug loading and release.

A versatile and simple methodology for fabricating microcapsules is by using a template.^[19–21] There are many templates used, such as weakly cross-linked melamine formaldehyde particles (MF), polystyrene particles (PS), MnCO_3 , CdCO_3 , and CaCO_3 .^[22] Especially uniform sized and porous CaCO_3 microparticles made from supersaturated solutions have been intensively studied and have found widespread application.^[23–27] CaCO_3 microparticles are biocompatible, inexpensive, and easy to produce and they decompose by complexation with ethylenediamine tetraacetic acid (EDTA) at neutral pH. Beside those merits, CaCO_3 microparticles offer a large surface area for adsorption of substances of interest due to their porous structure, which makes them an excellent carrier in drug release or as templates.^[28–30,50]

In this paper, we integrate the advantages of gelatin and porous CaCO_3 nanoparticles to fabricate gelatin microgels through a “casting” strategy. The process involves three steps: Firstly, a hot aqueous solution of gelatin is adsorbed by porous CaCO_3 at 50 °C. Secondly, the adsorbed gelatin is crosslinked by the natural cross-linker Genipin after addition of cold water. Thirdly, the cross-linked CaCO_3 -gelatin microparticles are treated by EDTA to obtain gelatin microgels. Herein, the porous CaCO_3 plays a role of “negative template”. Our method avoids employing organic solvents and surfactants, and a natural cross-linking agent is employed to reduce the possible side

Prof. J. C. M. van Hest
Institute for Molecules and Materials
Radboud University Nijmegen
Heyendaalseweg 135, 6525 AJ Nijmegen, The Netherlands
E-mail: j.vanHest@science.ru.nl

Prof. J. Li
Key Lab of Colloid and Interface Sciences
Institute of Chemistry
Chinese Academy of Sciences
Zhong Guan Cun, Bei Yi Jie 2, Beijing 100190, China
E-mail: jbli@iccas.ac.cn

Dr. A. Wang
Institute for Molecules and Materials
Radboud University Nijmegen
Heyendaalseweg 135, 6525 AJ Nijmegen, The Netherlands

Dr. Y. Cui
Key Lab of Colloid and Interface Sciences
Institute of Chemistry
Chinese Academy of Sciences
Zhong Guan Cun, Bei Yi Jie 2, Beijing 100190, China



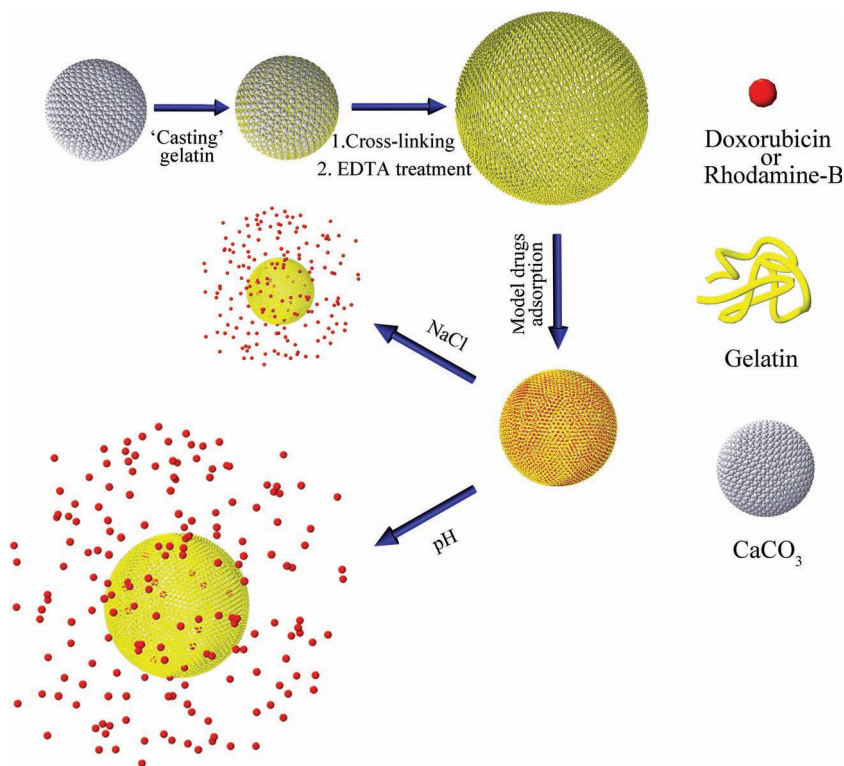
DOI: 10.1002/adfm.201102907

effects of residual cross-linker molecules. The gelatin microgels copy the loose and porous structure of CaCO_3 , which affords the gelatin microgels as a biocompatible, biodegradable and efficient delivery system.

2. Results and Discussion

2.1. Preparation of Gelatin Microgels by a Casting Strategy

Porous gelatin microspheres were prepared according to the procedure depicted in Scheme 1. First, as templates, CaCO_3 microparticles with diameters of 2.6 ± 0.3 and $4.7 \pm 0.3 \mu\text{m}$ (mean value \pm SD, $n = 50$) were obtained via adjusting the stirring time during the preparation procedure (Figure 1a,b). High resolution scanning electron microscopy (SEM) analysis showed that the surface of these porous particles was very rough and consisted of carbonate nanoparticles (about $40 \sim 70$ nm, estimated from Figure 1c). For the subsequent experiments the $4.7 \mu\text{m}$ microparticles were taken as templates. These CaCO_3 microparticles were incubated in a hot aqueous gelatin solution at 50°C for 6 hours, which allowed the protein to enter the pores of the CaCO_3 template. Upon addition of cold water at 4°C this process was stopped due to the increase in viscosity. Unadsorbed gelatin was removed by centrifugation. Figure 1c and d show the surface morphology of CaCO_3 before and after adsorption of gelatin, demonstrating that the rough surface was completely covered with gelatin. In the following step the gelatin- CaCO_3 microparticles were cross-linked in order to prevent the rapid dissolution of gelatin in aqueous solution. Many chemical and physical cross-linking methods have been developed for the preparation of gelatin nano- and microgels with long-term stability.^[3,7,35–38] In this research Genipin was employed. Genipin is a natural cross-linker obtained from geniposide, which can be isolated from the fruits of *Gardenia jasminoides* Ellis.^[1,2,9,39–42] Genipin can spontaneously react with amino acids or proteins to form dark blue pigments; the mechanism has been described in literature.^[2,40,41] It has been proposed that Genipin reacts with amino groups of gelatin to induce the cross-linking. Possible reaction mechanisms are shown in Scheme 2.^[2] The FDA-approved Genipin indeed proved to be a very useful cross-linker for the stabilization of the gel particles. Subsequently, the CaCO_3 template material was removed by treatment with EDTA. From the transmission



Scheme 1. Schematic illustration for the formation of gelatin microgels and their uptake and release of model drugs via salt and pH change.

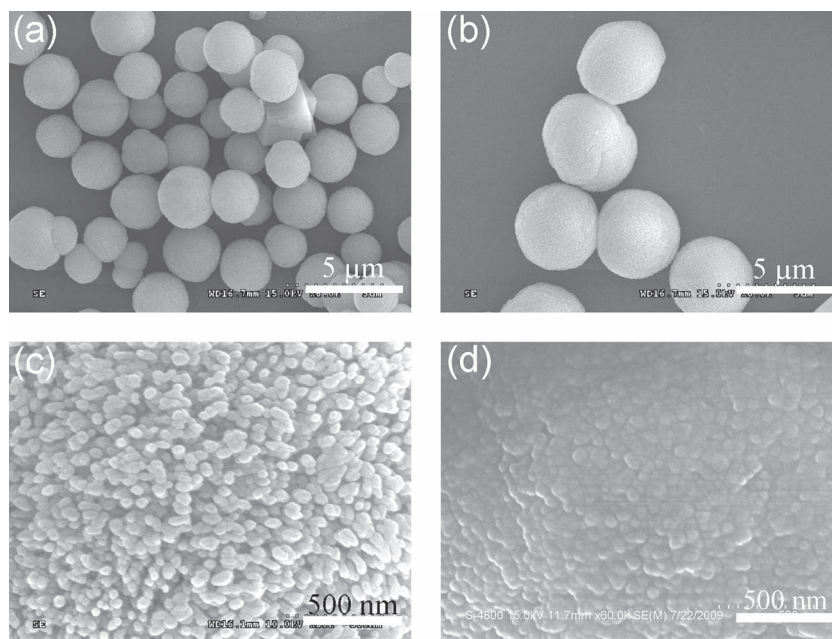
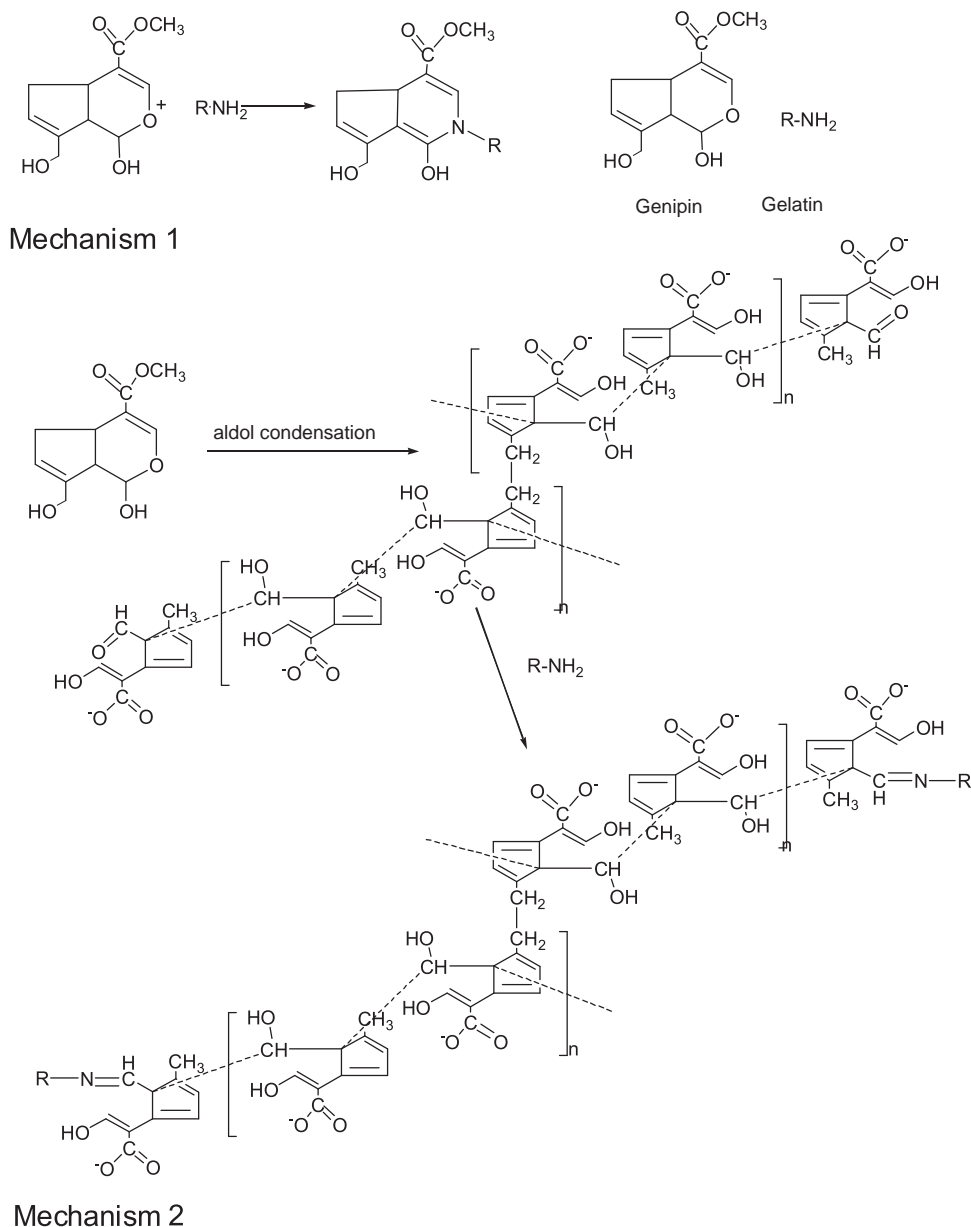


Figure 1. a,b) SEM images of CaCO_3 microparticles with different sizes; c,d) Surface morphology of CaCO_3 before (c) and after (d) adsorption of gelatin.

electron microscopy (TEM) and SEM images of the final particles, it was shown that both the size (Figure 2a and b) and the porous structure (Figure 2c) of the CaCO_3 templates (Figure 1b, $4.7 \mu\text{m}$) were to a considerable extent conserved in the gelatin



Scheme 2. The proposed mechanism of the reaction between Genipin and gelatin.^[2]

microgels ($5.1 \pm 0.4 \mu\text{m}$, mean value \pm SD, $n = 50$). Meanwhile, energy-dispersive X-ray spectra (EDX) confirmed that CaCO_3 was removed completely from the microparticles (Figure 2d). The templating role of CaCO_3 particles became even more clear when irregular particles were used, of which the morphology was copied by the gelatin microgels (Figure S1, Supplementary data).

To further certify the open structure of the microgels, atomic force microscopy (AFM) experiments were performed. It was estimated that the microgel thickness after drying was about $450 \pm 50 \text{ nm}$ (mean value \pm SD, $n = 80$, Figure 3a). This value is much smaller than that of the template diameter, indicating that the gelatin microgels were collapsed due to their loose structure. Meanwhile, from Figure 3b, the pore

size on the surface of the microgels was estimated to be about $20 \sim 60 \text{ nm}$, which is somewhat smaller than the size of the carbonate nanostructures ($40 \sim 70 \text{ nm}$). Confocal laser scanning microscopy (CLSM) images (Figure 3c) showed the gelatin microgels had an intrinsic fluorescence and were excited by 488 and 559 nm laser light. This is likely due to the formation of the pyridine-like structures after the primary amine groups on gelatin reacted with Genipin (shown in Scheme 2), and intrinsic chromophoric groups of gelatin.^[43,44] This property facilitates to trace the distribution of the microgels in biological systems. Additionally, the diameter was estimated to be about $9.0 \pm 0.8 \mu\text{m}$ (mean value \pm SD, $n = 30$), (gelatin microgels with a diameter of $4.1 \pm 0.43 \mu\text{m}$ were observed when the $2.6 \mu\text{m}$ CaCO_3 microparticles were taken as template Figure S2,

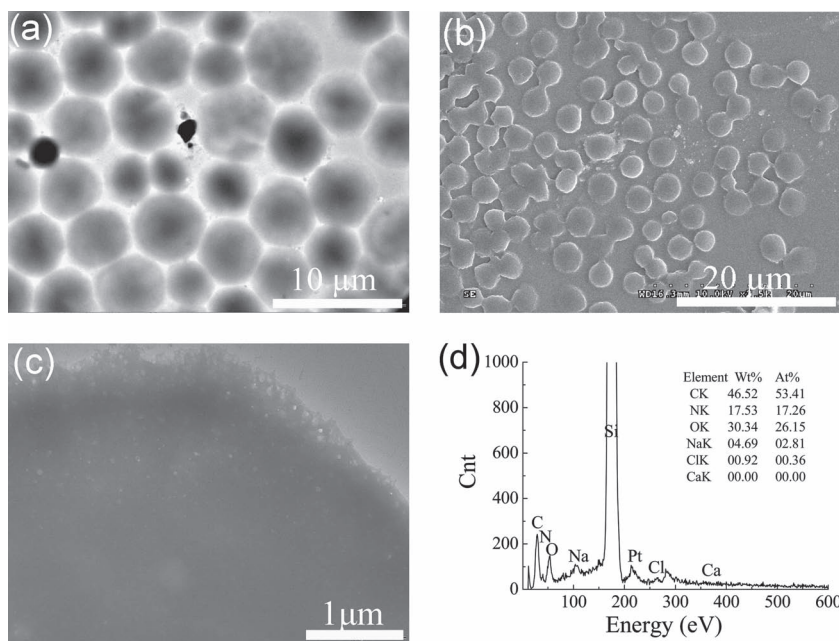


Figure 2. a) TEM images of gelatin microgels derived from CaCO_3 ; b) SEM; c) Magnified TEM images; d) EDX spectrum of the gelatin microgels.

Supplementary data). Besides the fact that different techniques will slightly under- or overestimate particle size, the increase in size compared to the electron microscopy (EM) measurements can in this case also be attributed to the adsorption of water, which causes swelling of the gelatin microgels.^[9] From the fluorescence intensity, the loose structure of the microgel could be seen clearly (Figure 3c insert). The inner part of the microgel had a lower gelatin density than the shell part, which confirms the results of electron microscopy.

2.2. The Salt and pH Responsiveness of Gelatin Microgels

The relationship between the zeta potential of gelatin microgels and pH values is shown in Figure 4a. In the range of pH 3.0–7.4, the gelatin microgels possessed a negative zeta potential which changed from –3.7 to –13.1 mV. This negative value is a result of the fact that most amino groups of gelatin (from arginine and lysine) were consumed due to cross-linking with Genipin, and carboxylic acid groups were left (from aspartic acid and glutamic acid), which are responsible for the negative charge of microgels due to deprotonation upon increasing pH. The diameter of the gelatin microgels also changed along with the pH, Figure 4b shows the diameter increased as the pH increased (from 3 to 7 μm). It is deduced

that internal charge repulsion within gelatin microgels caused this phenomenon. CLSM images illustrate this process (Figure 4b inserts).

It has been reported that microgels can respond to many environmental stimuli (such as temperature, salt concentration, light, etc.).^[45–49] Here, the obtained gelatin microgels were incubated in NaCl solution to investigate the effect of salt concentrations. In aqueous solution, the diameter was estimated to be about $9.0 \pm 0.8 \mu\text{m}$, however, it changed to a mean diameter of $5.4 \pm 0.4 \mu\text{m}$ in 1 M NaCl solution (Figure 5) within several seconds after addition of salt. The microgel shrinkage is likely a result of reduced osmotic pressure inside the microgels; this is due to the charge shielding effect of salt on the negatively charged functional groups.^[46–48]

The repeatability of responding to stimuli is a very important aspect if one wants to consider the use of the microgels for drug loading and release. To test this property, the same microgels were incubated in NaCl solution (0.2 M) and water alternately. Figure 6 displays six cycles and shows that the diameter of microgels recovered to the original size after replacing the NaCl solution with Milli-Q water. This demonstrates the good repeatability of salt responsiveness of the microgels.

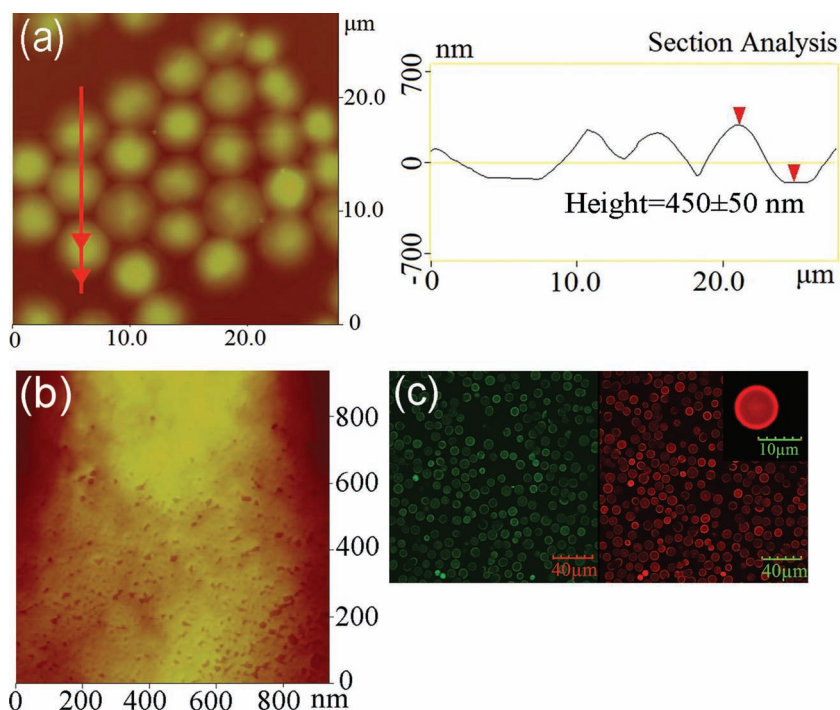


Figure 3. a) AFM images of gelatin microgels; b) the corresponding surfaces for an indicated area with a size $0.9 \mu\text{m} \times 0.9 \mu\text{m}$; c) CLSM (excited by 488, 559 nm laser light) images, insert: magnification.

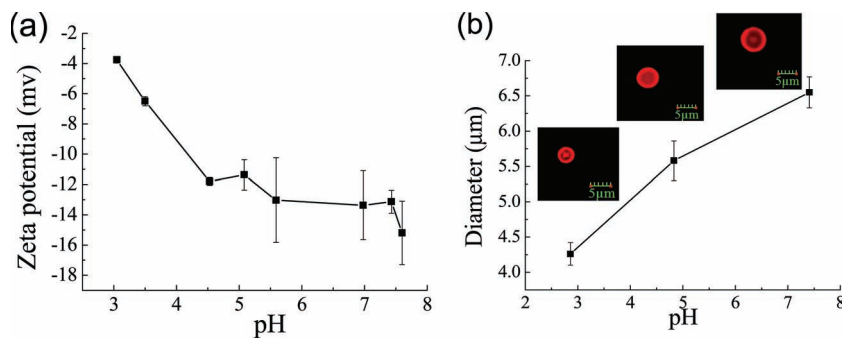


Figure 4. Gelatin microgels: a) The zeta potential of gelatin microgels in different pH solutions; b) The changes of diameter and CLSM images of gelatin microgels in different pH buffer solutions.

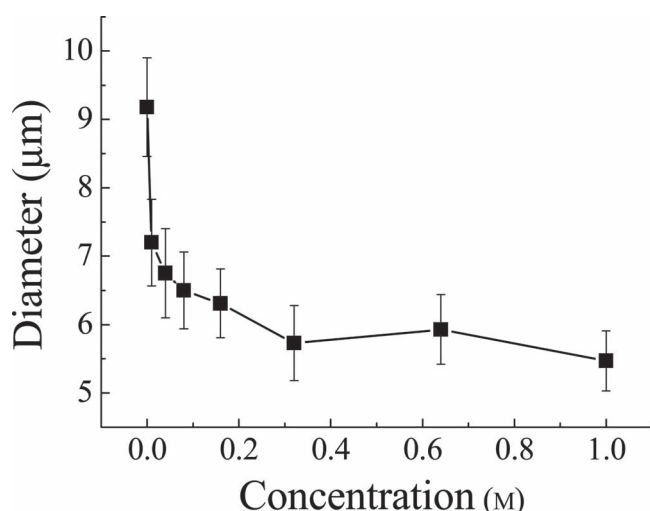


Figure 5. The changes of diameter in different concentrations of NaCl.

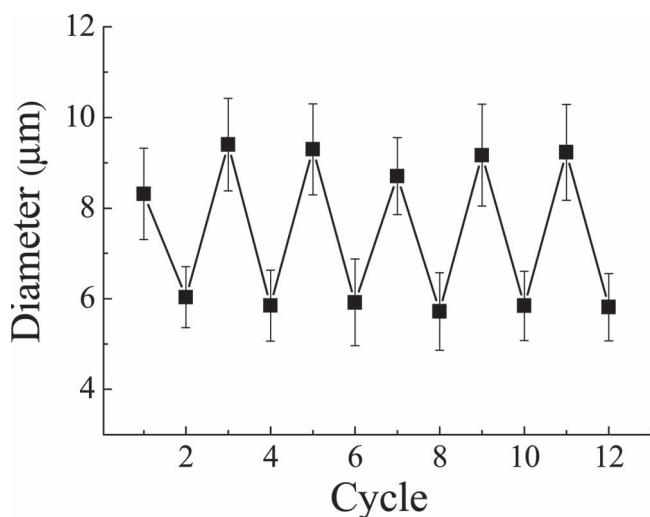


Figure 6. Repeatability of salt responsiveness of gelatin microgels. (Odd number: In deionized water. Even number: In 0.2 M NaCl solution).

2.3. The Uptake Capability of Gelatin Microgels for Molecules with Different Charge

Gelatin microgels with a porous and loose structure are expected to have a good loading capability for positively charged molecules. Molecules with different charge were employed to investigate this feature. Firstly, 6-CF (5(6)-carboxyfluorescein, $M_w \sim 376.32 \text{ g mol}^{-1}$), a negatively charged molecule, was chosen to test the effect of charge. Aqueous solutions with low concentrations of 6-CF were prepared to avoid the permeability change caused by osmotic pressure; The CLSM images in Figure 7a indicate the molecule was excluded by gelatin microgels due to

electrostatic repulsion at any concentration. In contrast, acridine orange with a similar molecular weight ($M_w \sim 396.96 \text{ g mol}^{-1}$) but a positive charge quickly diffused into the gelatin microgels (Figure 7b) at low concentration. It is concluded that gelatin microgels can load small molecules with positive charge spontaneously and repulse molecules with negative charge.

It was expected that the permeability will be changed in response to the alteration of the diameter of the microgels. Acridine orange was chosen as a probe molecule to investigate the change of permeability. Gelatin microgels possess negative charge; therefore, the addition of acridine orange first will result in accumulation inside the gel particles due to electrostatic interactions and a shielding of the repulsive forces, leading to smaller particles. CLSM images in Figure 8 show the relationship between the microgel's diameter and concentration of acridine orange. Herein, a 488 nm laser was applied to facilitate the investigation of the changes of diameter and permeability of the microgels. The diameter changed from 8.3 ± 1.0 to $3.6 \pm 0.4 \mu\text{m}$ as the concentration increased from 0 to $4.6 \times 10^{-4} \text{ M}$. It is believed that the mechanism is similar to that of NaCl. As expected, the permeability of microgels changed following the decrease in diameter. The microgels excluded acridine orange at a concentration of $2.3 \times 10^{-4} \text{ M}$ with a diameter of $3.8 \mu\text{m}$. This property offers an opportunity to control the encapsulation and release of drugs by osmotic pressure.

2.4. The Spontaneous Loading and Release of Doxorubicin by Salt Concentration

Doxorubicin, a positively charged anticancer drug, was chosen to investigate drug uptake and release from gelatin microgels. Microscopy images (Figure 9a, b) confirmed that the gelatin microgels became opaque after adsorption of Doxorubicin, compared to the transparent ones before adsorption. It was found that the loading efficiency reached 90% when the initial concentration of Doxorubicin was 0.1 mg mL^{-1} . It is known that salt strength has a big effect on the electrostatic interaction between microgels and model drugs, therefore, the Doxorubicin-loaded gels were incubated in 0.2 M NaCl solution to investigate release behavior of the model drug. Figure 9c displays typical time-dependent release curves. In the case without salt, the Doxorubicin released slowly from gelatin microgels, and the

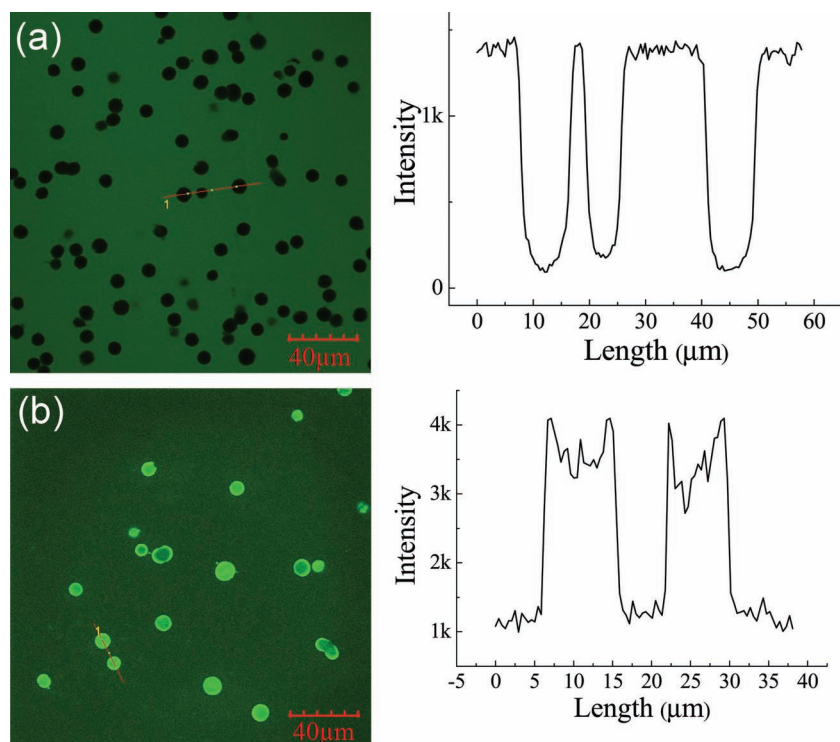


Figure 7. The upload capability of microgels for a) 5(6)-Carboxyfluorescein (MW ~ 376.32 g mol⁻¹); b) Acridine orange (MW ~ 396.96 g mol⁻¹).

release process lasted for about 8 hours after which about 90% of adsorbed Doxorubicin was released. In contrast, in 0.2 M NaCl solution, about 56% of Doxorubicin released from gelatin microgels within 10 minutes. It is reasonable to believe that the charge shielding effect caused by NaCl, which reduced the interaction between gelatin microgels and Doxorubicin, triggered the fast drug release from microgels. On the other hand, the large and fast diameter change (diameter decrease, 34% in 0.2 M NaCl solution in several seconds) in this process may also contribute to the burst drug release in salt medium.

2.5. Rhodamine B Release Controlled by pH

The interaction between microgels and model drugs at different pH (1.2 and 7.4) was investigated via the release of the Rhodamine B model drug from the microgels. The values were chosen to mimic the pH in the stomach (1.2) and under physiological conditions (7.4), respectively. It was expected that the gelatin microgels could keep the payload at acidic conditions and release them at neutral to basic pH. Rhodamine B was employed as a model drug because of its positive charge and low molecular weight. As shown in the release profile (Figure 10), the rate of release was very slow in the pH 1.2 solution, just about 30% of the payload released from the gelatin microgels in the course of 3 hours; in contrast, as much as 90% of the payload was released in the pH 7.4 buffer solution during the same time period. An explanation is that the permeability of gelatin microgels is low as there is low charge repulsion in a pH 1.2 solution, which therefore keeps the payload

inside. As the microgels are almost neutral at pH 1.2, there is little interaction with the positively charged model drugs, (Figure 4a), so the low permeability of microgels plays a main role for the slow drug release at pH 1.2. After increasing the pH to 7.4, Rhodamine B becomes neutral, and there is no interaction between model drugs and microgel since the latter one becomes negatively charged due to deprotonation of the carboxyl acid groups. However, the permeability of the microgels increases because of high charge repulsion, which therefore allows the release of Rhodamine B from the microgels more quickly. Additionally, the microgels are very stable in this process; the microgels kept their shape in pH 1.2 HCl solution for more than one week (as shown in Figure S3, Supplementary data). It can be concluded that drug release can be controlled by changes in pH or ionic strength of the medium. Gelatin microgels can therefore possibly protect fragile drugs from undesired interactions with gastric fluids and release them as they reach the intestine.

Biodegradability and biocompatibility are essential for materials which are used as

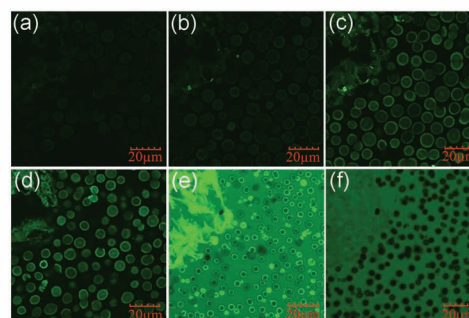
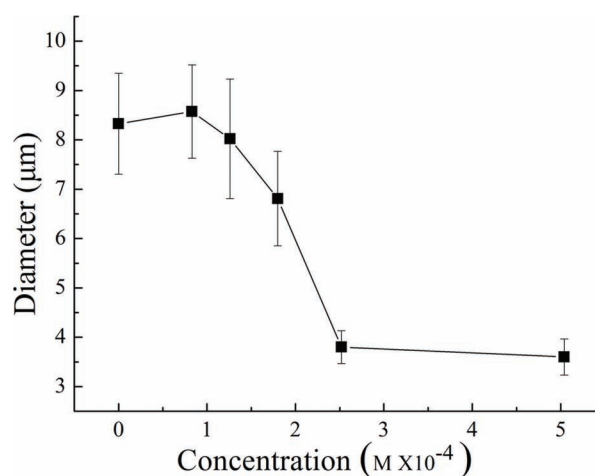


Figure 8. The changes of the permeability and diameter of gelatin microgels in response to different concentrations of acridine orange: a) 0, b) 0.83×10^{-4} , c) 1.26×10^{-4} , d) 1.8×10^{-4} , e) 2.5×10^{-4} , f) 5.0×10^{-4} M.

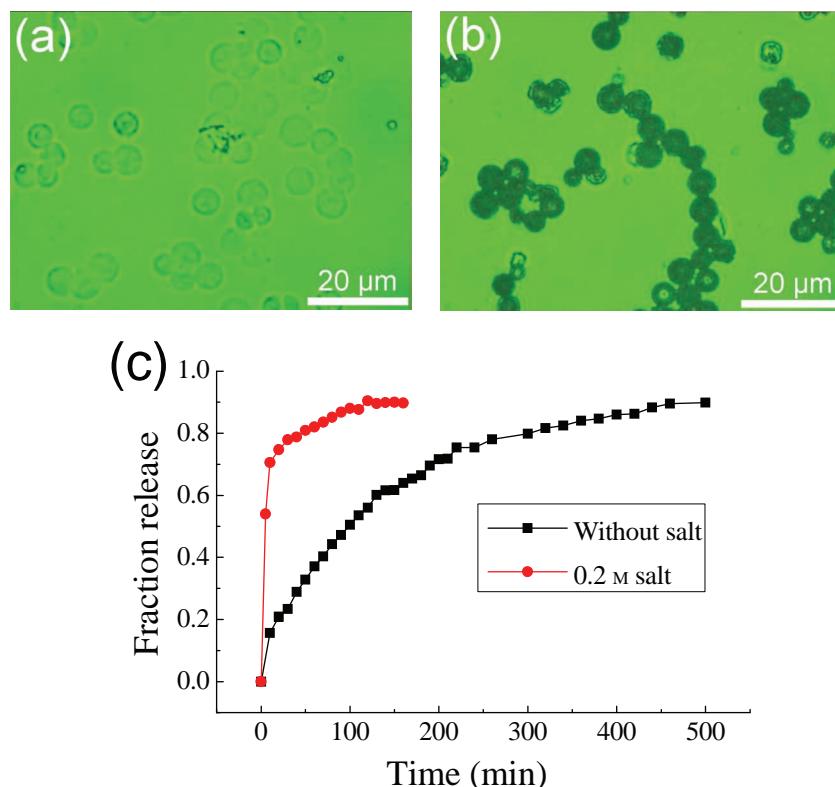


Figure 9. Microscopy images of gelatin microgels a) before, b) after loading with doxorubicin. c) The release profile of loaded doxorubicin from gelatin microgels in different concentrations of NaCl.

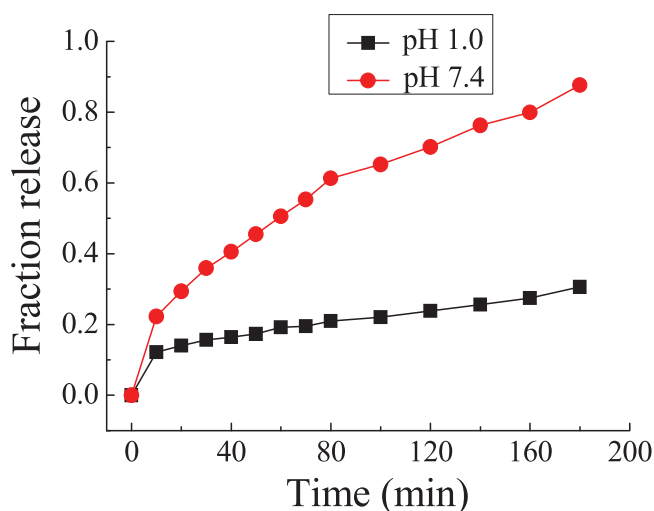


Figure 10. The release profile of loaded Rhodamine B in response to pH.

drug vehicle. To certify their biodegradability the gelatin microgels were incubated in a highly concentrated trypsin solution (1 wt%). CLSM images (Figure S4, Supplementary data) show that the gelatin microgels started to be digested quickly, and the bulk of the gelatin microgels disappeared after 120 minutes. This suggests that gelatin microgels can be accessible for

trypsin despite of the Genipin cross-linking. Cell experiments also confirmed that the gelatin microgels were taken up by human breast adenocarcinoma cells (MCF-7) with low cytotoxicity (Figure S5, Supplementary data).

Note: The supplementary data contains the following additional material. Figure S1 displays SEM images of microgels which copied the structure of irregularly shaped CaCO_3 particles. Figure S2 shows CLSM images of gelatin microgels derived from $2.6 \pm 0.25 \mu\text{m}$ CaCO_3 . Figure S3 proves the stability of microgels in 1.2 and 7.4 buffer solutions. Figure S4 and 5 demonstrate that the microgels have a good biodegradability and can be taken up by HeLa cells with low cytotoxicity.

3. Conclusions

Highly intrinsic fluorescent, uniform and stable gelatin microgels with a porous structure have been prepared via a “casting” strategy using CaCO_3 particles as negative template. The procedure is very simple and involves no organic solutions or surfactants. The diameter of the obtained negatively charged gelatin microgels is dependent on the size of the CaCO_3 microparticles. The microgels copy the porosity of CaCO_3 templates with pore sizes of about 20 ~ 60 nm in the dry state. The diameter and permeability of gelatin microgels are sensitive to salt concentration and pH. Small molecules with positive charge, such as Doxorubicin and Rhodamine B can be adsorbed spontaneously by the negatively charged gelatin microgels. Meanwhile, the release of these molecules can be controlled by the salt concentration and pH. Additionally, biodegradability and biocompatibility were demonstrated by digestion by trypsin of gelatin microgels and their uptake by HeLa cells, showing low cytotoxicity.

4. Experimental Section

Materials: Gelatin (Viscosity dynamic: 1.5–6.0 mPa) was obtained from Merck KGaA (Germany). Acridine orange ($\text{Mw} \sim 396.96 \text{ g mol}^{-1}$), Rhodamine B ($\text{Mw} \sim 479.02 \text{ g mol}^{-1}$) 5(6)-Carboxyfluorescein ($\text{Mw} \sim 376.32 \text{ g mol}^{-1}$), and Doxorubicin ($\text{Mw} \sim 579.99 \text{ g mol}^{-1}$) were purchased from Sigma-Aldrich. Gelatin was used without further purification and prepared as a 15 wt% solution at 50 °C. Genipin was obtained from Wako Company (Japan). The water used in all experiments was prepared in a three-stage Millipore Milli-Q plus 185-purification system and had a resistivity higher than 18.2 MΩ.

Fabrication of Size-Tunable CaCO_3 : Porous CaCO_3 microparticles with a tunable size were synthesized by mixing CaCl_2 and Na_2CO_3 solutions according to improved literature procedures.^[28–34] In a typical experiment, 0.615 mL (0.33 M) Na_2CO_3 was poured in to a solution of 0.615 mL CaCl_2 (0.33 M), and the mixture was intensely agitated on a magnetic stirrer (1200 rpm min^{-1}) with stirring times of 20 s or 40 s. The prepared microparticles were washed with deionized water thoroughly for three times.

Preparation of Gelatin Microgels by a "Casting" Strategy: For the preparation of gelatin microgels, different sized CaCO_3 microparticles were gently shaken with 2 mL aqueous gelatin solution (15 wt%) at 50 °C for 6 hours to achieve pore saturation. Then, 8 mL deionized water at 4 °C was poured into the mixture quickly. After two centrifugation/water rinsing/redispersion cycles, 2 mL Genipin solution (0.028 M) was added to cross-link gelatin at room temperature; the reaction was continued for 16 hours to ensure complete conversion. Then, the samples were centrifuged, rinsed by water and redispersed for three times. The gelatin microgels were obtained by treatment of cross-linked CaCO_3 -gelatin with EDTA (0.1 M, pH 7.0), following the procedure in previous studies.^[28,30]

The Effect of Salt Concentration and pH on the Diameter and Permeability of Gelatin microgels: An aqueous dispersion of gelatin microgels was added to a Petri dish. After the microgels had settled on the bottom of the dish, most of the supernatant solution was removed carefully using a pipette. Next, different concentrations of NaCl solution with acridine orange, sodium citrate-hydrochloric acid (pH 3.0, 4.8, 0.01 M) or PBS (7.4, 0.01 M) buffer solution were added. The samples were observed at appropriate time intervals by CLSM.

Uptake and Release of Doxorubicin and Rhodamine B by Gelatin Microgels: The uptake of Doxorubicin and Rhodamine B was achieved by incubating 1 mL microgels (about 9×10^7 particles mL^{-1} , determined by cell counting chamber) in 1 mL Doxorubicin or Rhodamine B solution (0.1 mg mL^{-1}) for 6 hours. Thereafter, the microgels were separated by centrifugation, rinsed by water and redispersed for three times to remove the unbound Doxorubicin or Rhodamine B. UV-vis spectroscopy was employed to estimate the loading efficiency.

The gelatin microgels loaded with Doxorubicin or Rhodamine B were incubated in 1.5 mL of different concentrations of NaCl (0, 0.2 M, at room temperature), PBS buffer solution (pH 7.4, at 37 °C) or HCl solution (pH 1.2, at 37 °C, with the same ionic strength of PBS). Then 0.5 mL of the supernatant was taken out each time from the system, whilst supplementing the same volume of water, NaCl solution or buffer solution to keep the total volume constant at 1.5 mL. The characteristic absorbance of Doxorubicin or Rhodamine B was recorded. The cumulative released amount was calculated for each measurement with concentrations determined from a calibration curve.

Characterization of the CaCO_3 Microparticles and Gelatin microgels: UV-visible spectra (UV-vis) were recorded with a HITACHI U-3010 UV-visible spectrophotometer. The transmission electron microscopy (TEM) microscopy images were acquired by using a Philips CM200-FEG instrument. Energy-dispersive X-ray spectra (EDX) were obtained from an S-4800 instrument with 10 kV accelerating voltage. Digital Instrument Nanoscopy III (AFM) was used to obtain micrographs of microcapsules in the tapping mode at room temperature. Scanning electron microscopy (SEM) was performed with a HITACHI S-4300 apparatus (HITACHI, Japan). The fluorescence images of microcapsules were taken by an Olympus FV500 scanning device (Olympus, Japan).

Supporting Information

Supporting Information is available from the Wiley Online Library or from the author.

Acknowledgements

The authors thank NanoNextNL for financial support.

Received: November 30, 2011

Revised: February 13, 2012

Published online: March 30, 2012

- [1] A. J. Kuijpers, P. B. van Wachem, M. J. A. van Luyn, J. A. Plantinga, G. H. M. Engbers, J. Krijgsveld, S. A. J. Zaat, J. Dankert, J. Feijen, *J. Biomed. Mater. Res.* **2000**, 51, 136.
- [2] H. C. Liang, W. H. Chang, H. F. Liang, M. H. Lee, H. W. Sung, *J. Appl. Polym. Sci.* **2004**, 91, 4017.

- [3] J. Eysturskarð, I. J. Haug, N. Elharfaoui, M. Djabourov, K. I. Draget, *Food Hydrocolloids* **2009**, 23, 1702.
- [4] X. H. Liu, P. X. Ma, *Biomaterials* **2009**, 30, 4094.
- [5] S. Sakai, K. Hirose, K. Taguchi, Y. Ogushi, K. Kawakami, *Biomaterials* **2009**, 30, 3371.
- [6] R. Yin, Y. Q. Huang, C. J. Huang, Y. J. Tong, N. Tian, *Mater. Lett.* **2009**, 63, 1335.
- [7] M. A. Vandelli, M. Romagnoli, A. Monti, M. Gozzi, P. Guerra, F. Rivasi, F. Forni, *J. Controlled Release* **2004**, 96, 67.
- [8] T. Coviello, P. Matricardi, C. Marianecci, F. Alhaique, *J. Controlled Release* **2007**, 119, 5.
- [9] H. C. Liang, W. H. Chang, K. J. Lin, H. W. Sung, *J. Biomed. Mater. Res.* **2003**, 65A, 271.
- [10] J. K. Oh, D. I. Lee, J. M. Park, *Prog. Polym. Sci.* **2009**, 34, 1261.
- [11] J. K. Oh, R. Drumright, D. J. Siegwart, K. Matyjaszewski, *Prog. Polym. Sci.* **2008**, 33, 448.
- [12] A. Khademhosseini, R. Langer, *Biomaterials* **2007**, 28, 5087.
- [13] A. Fernández-Barbero, I. J. Suárez, B. Sierra-Martín, A. Fernández-Nieves, F. Javier de las Nieves, M. Marquez, J. Rubio-Retama, E. López-Cabarcos, *Adv. Colloid Interface Sci.* **2009**, 147–148, 88.
- [14] Y. Lu, *Sci. Technol. Gelatin* **2006**, 26, 113.
- [15] Z. Gu, L. Kong, X. Feng, T. Guo, J. Dai, S. Li, N. Huo, Y. Ding, *J. Alloys Compd.* **2009**, 474, 450.
- [16] A. W. Maki, W. E. Bishop, *Arch. Environ. Contam. Toxicol.* **1979**, 8, 599.
- [17] P. M. Williams, G. Payne, *Royal Society of Chemistry & EOSCA. Manchester* **2001**. Available from URL: <http://www.eosca.com/docs/Surfactants%20Report.pdf> (accessed March, 2012)
- [18] P. Arien-Søborg, L. Henriksen, A. Gade, C. Gyldensted, O. B. Paulson, *Acta Neurologica Scandinavica* **1982**, 66, 34.
- [19] Q. He, Y. Cui, J. B. Li, *Chem. Soc. Rev.* **2009**, 38, 2292.
- [20] Q. He, L. Duan, W. Qi, K. W. Wang, Y. Cui, X. H. Yan, J. B. Li, *Adv. Mater.* **2008**, 20, 2933.
- [21] Q. He, S. Ai, Y. Tian, J. B. Li, *Curr. Opin. Colloid Interface Sci.* **2009**, 14, 115.
- [22] A. A. Antipov, D. Shchukin, Y. Fedutik, A. I. Petrov, G. B. Sukhorukov, H. Möhwald, *Colloids Surf., A* **2003**, 224, 175.
- [23] N. Koga, Y. Nakagoe, H. Tanaka, *Thermochimica Acta* **1998**, 318, 239.
- [24] S. L. Tracy, D. A. Williams, H. M. Jennings, *J. Cryst. Growth* **1998**, 193, 382.
- [25] D. Horn, J. Rieger, *J. Angew. Chem. Int. Ed. Engl.* **2001**, 40, 4330.
- [26] M. Kitamura, *J. Colloid. Interface Sci.* **2001**, 236, 318.
- [27] M. Kitamura, H. Konno, A. Yasui, H. Masuoka, *J. Cryst. Growth* **2002**, 236, 323.
- [28] D. V. Volodkin, A. I. Petrov, M. Prevot, G. B. Sukhorukov, *Langmuir* **2004**, 20, 3398.
- [29] G. B. Sukhorukov, D. V. Volodkin, A. M. Günther, A. I. Petrov, D. B. Shenoy, H. Möhwald, *J. Mater. Chem.* **2004**, 14, 2073.
- [30] D. V. Volodkin, N. I. Larionova, G. B. Sukhorukov, *Biomacromolecules* **2004**, 5, 1962.
- [31] W. Wei, G. Ma, G. Hu, D. Yu, T. Mcleish, Z. G. Su, Z. Y. Shen, *J. Am. Chem. Soc.* **2008**, 130, 15808.
- [32] C. Y. Wang, C. Y. He, Z. Tong, X. X. Liu, B. Ren, F. Zeng, *Int. J. Pharm.* **2006**, 308, 160.
- [33] Y. Ueno, H. Futagawa, Y. Takagi, A. Ueno, Y. Mizushima, *J. Controlled Release* **2005**, 103, 93.
- [34] Q. H. Zhao, S. Zhang, W. J. Tong, C. Y. Gao, J. C. Shen, *Eur. Polym. J.* **2006**, 42, 3341.
- [35] R. Cortesi, E. Esposito, M. Osti, E. Menegatti, G. Squarzon, S. S. Davis, C. Nastruzzi, *Eur. J. Pharm. Biopharm.* **1999**, 47, 153.
- [36] T. D. Weatherill, R. W. Henning, K. Smith, *J. Photogr. Sci.* **1992**, 40, 220.
- [37] R. Cortesi, C. Nastruzzi, S. S. Davis, *Biomaterials* **1998**, 19, 1641.

- [38] K. Terao, T. Karino, N. Nagasawa, F. Yoshii, M. Kubo, T. Dobashi, *J. Appl. Polym. Sci.* **2004**, 91, 3083.
- [39] A. Bigi, G. Cojazzi, S. Panzavolta, N. Roveri, K. Rubini, *Biomaterials* **2002**, 23, 4827.
- [40] C. H. Yao, B. S. Liu, C. J. Chang, S. H. Hsu, Y. S. Chen, *Mater. Chem. Phys.* **2004**, 83, 204.
- [41] K. S. Huang, K. Lu, Ch. S. Yeh, S. R. Chung, C. H. Lin, C. H. Yang, Y. S. Dong, *J. Controlled Release* **2009**, 137, 15.
- [42] M. T. Nickerson, R. Farnworth, E. Wagar, S. M. Hodge, D. Rousseau, A. T. Paulson, *Int. J. Biol. Macromol.* **2006**, 38, 40.
- [43] F. L. Mi, *Biomacromolecules* **2005**, 6, 975.
- [44] W. G. Liu, K. D. Yao, G. C. Wang, H. X. Li, *Polymer* **2000**, 41, 7589.
- [45] Q. Zhou, B. J. Chu, *J. Phys. Chem. B.* **1998**, 102, 1364.
- [46] B. H. Tan, K. C. Tam, *Adv. Colloid Interface Sci.* **2008**, 136, 25.
- [47] M. J. Snowden, B. Z. Chowdhry, B. Vincent, G. E. Morris, *Chem. Soc., Faraday Trans.* **1996**, 92, 5013.
- [48] B. H. Tan, K. C. Tam, Y. C. Lam, C. B. Tan, *Langmuir* **2004**, 20, 11380.
- [49] B. M. Budhlall, M. Marquez, O. D. Velev, *Langmuir* **2008**, 24, 11959.
- [50] D. V. Volodkin, R. von Klitzing, H. Möhwald, *Angew. Chem. Int. Ed.* **2010**, 49, 9258.